RSC Advances

PAPER

Cite this: *RSC Adv.*, 2015, **5**, 5158

Probing a dip-coated layer of organic molecules by an aerosol nanoparticle sensor with sub-100 nm resolution based on surface-enhanced Raman scattering†

Masao Gen[a] and I. Wuled Lenggoro*[ab]

A surface coated with organic molecules has been probed by a sub 100 nm resolution particulate sensor by surface-enhanced Raman scattering (SERS) technique. The spatial distribution of those molecules formed on the solid surface was altered by a dip-coating method as a function of a substrate-lifting rate. Isolated silver nanoparticles (~50 nm) as "antenna" particles were deposited from the gas phase onto the surface by means of an electrostatic-assisted spray. The surface with the particles was analyzed with Raman spectroscopy technique. These analyses provide spatial information on the molecules over the surface, when SERS spectra of the molecules obtained from each measurement point are converted into the position of molecules. The occurrence frequency of SERS is found to be correlated with the two-third power law of the lifting rate which is proportional to a mass concentration of molecules per unit area, whereas the average Raman intensity is independent. A gas-phase route assisted SERS technique offers direct measurement of the molecular patterns on target surfaces.

Received 27th April 2014
Accepted 11th December 2014

DOI: 10.1039/c4ra03850a

www.rsc.org/advances

Introduction

A variety of analytical techniques have been developed to characterize the surface properties of organic/inorganic materials;[1–3] such as, vacuum techniques (X-ray photoelectron spectroscopy and Auger electron spectroscopy), optical spectroscopies (IR and Raman spectroscopies), and scanning probe microscopies (Scanning tunneling microscopy and Atomic force microscopy). Unlike the vacuum techniques, Raman spectroscopy has been used at normal pressure in order to identify the chemical distribution on solid surfaces.[4] Further, this technique has accelerated a driving force to expand its practical applications with the availability of plasmonic metal nanoparticles that act as enhancer of Raman signals (*e.g.* for detection of pesticide residues in food).[5,6] The advantage with these enhancer nanoparticles relies on surface-enhanced Raman scattering (SERS) that has been studied since its recognition,[7,8] and provides sensitive characterization up to single-molecule detection.[9,10]

A SERS technique has shown its potential as a "fast" measure,[5,6] compared to the other separation-based methods (*e.g.* chromatography) that provide qualitative and quantitative analyses at part per billion levels[11] involving multiple procedures for sample preparations. In a typical case of SERS technique, however, a liquid sample including target molecules is used as a starting material.[12–14] If target molecules already exist in/on a surface (*e.g.* food crop and vegetation), it is necessary to transfer them from the solid to the liquid phase, possibly leading to the changes in the surface properties (*e.g.* spatial distributions and orientations of molecules on a surface). To give the SERS technique more practical features, the direct characterization of surface properties without an additional procedure on "surface-to-liquid" transfer offers a more desirable way to measure the "original" information.

Recently, surfaces (fruit peels) contaminated by probed molecules was directly analyzed by depositing a drop containing metal nanoparticles (colloidal suspension) on the surface of the peel.[5,15] This approach successfully measured Raman spectra of the molecules at particle/molecules/substrate interfaces, but it was necessary for the surface to be exposed to a liquid phase, eventually leading to missing data of the original condition of molecular distribution over the surface. If metal nanoparticles in the dry state were deposited, the approach could be greatly improved.

This study proposes gas-phase deposition of Ag nanoparticles (which act as 'antenna' particles), instead of colloidal deposition for SERS analysis. First, we focus on the applicability of the method using a model solid substrate *i.e.* silicon substrate. Dried Ag particles were uniformly dispersed over

[a]*Graduate School of Bio-Applications and Systems Engineering (BASE), Tokyo University of Agriculture and Technology, Koganei, Tokyo 184-8588, Japan. E-mail: wuled.@cc.tuat.ac.jp*

[b]*Department of Chemical Engineering, Tokyo University of Agriculture and Technology, Koganei, Tokyo 184-8588, Japan*

† Electronic supplementary information (ESI) available. See DOI: 10.1039/c4ra03850a

surfaces coated with target molecules by means of an electrostatic spray. This spray method generates highly charged nanoparticles in gas phase, and compulsively deposits them on target surfaces under given electric fields. SERS analysis in the presence of the antenna particles provided a spatial distribution of target molecules over surfaces. The distribution was altered by a dip-coating method.

Experimental

Material

A solution of clothianidin (one of neonicotinoid pesticides) was prepared at a concentration of 100 ppm in a water sample as target molecules. A surface of silicon wafer (100) with a dimension of 10 × 10 mm^2 was selected as a model one. Ag nanoparticles were synthesized by following the reduction method:[16] 90 mg of silver nitrate powder (Wako Pure Chemical Industries, Osaka) was dissolved with ultrapure water (500 mL) in a 500 mL glass beaker; This solution was heated up to around 94 °C with stirring at 500 rpm; A solution of 1% sodium citrate (10 mL, Wako Pure Chemical Industries, Osaka) was then added; The mixed solution was maintained at 94 °C for 1 hour, leading to particle formation. The prepared particles (suspension) were analyzed with dynamic light scattering (HPPS, Malvern Instruments, Worcestershire) for the size distribution and UV-vis NIR spectrometer (MSV-370, Jasco, Tokyo) for the optical property. The particle size and absorption peak measured were around 80 nm and 450 nm, respectively. The suspension was diluted with ethanol by a factor of 2 (water-to-ethanol ratio = 50 : 50) to decrease in surface tension of the liquid.

Coating of solid surface with organic molecules

A dip coating of a solid substrate with the pesticide solution was conducted with a motor of an infusion pump (KDS 100, KD Scientific, Holliston) at room temperature (20–25 °C) and relative humidity of 40%. The substrate was positioned perpendicularly to the liquid level of the solution. A substrate-lifting rate was varied at 1, 5, 10, 50 and 100 μm s^{-1} in order to alter a spatial distribution of target molecules on the surface (Fig. 1). The lifting rate at the speed of 1 μm s^{-1} required approximately 3 hours for moving in a 10 mm-vertical length of the substrate. No change in the liquid level was visually confirmed for the time period so that the evaporation from the bulk liquid surface can be neglected. The coated substrate was left for 1 hour at room temperature and controlled relative humidity to further evaporate the liquid film formed on the surface, resulting in the solid film (Fig. 1).

Deposition of Ag nanoparticles

An electrostatic spray that we developed (detailed configuration is presented in the ESI†) was used to deposit gas-phase Ag nanoparticles on the coated surfaces for spraying time of 1 hour. We used a single stainless (SUS304) spray nozzle with inner and outer diameter of 0.1 and 0.25 mm, respectively. The spray nozzle was applied with ~2.3 kV and a distance between

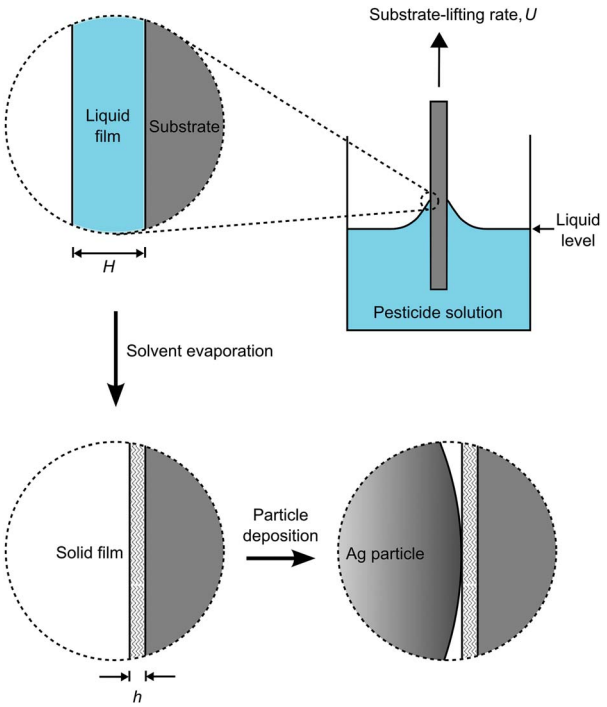

Fig. 1 A schematic illustration of coating of solid surface with organic molecules.

the nozzle and a substrate surface was maintained at 90 mm. A substrate was amounted on a metal-made stage with cylindrical shape and 15 mm diameter and the stage was applied with −1.0 kV to improve deposition efficiency. A suspension was supplied through the nozzle at flow rate of 0.2 mL h^{-1}.

Fig. 2 shows the size distribution of the deposited particles after a 1 hour spray being calculated from the electron micrograph of particles taken by a field-emission scanning electron microscope (JSM-633OFS, JEOL, Tokyo). The micrograph was analysed with an image processing software (ImageJ, National Institutes of Health, Bethesda). This analysis gives the average particle size of around 50 nm on the basis of the fitting curve,

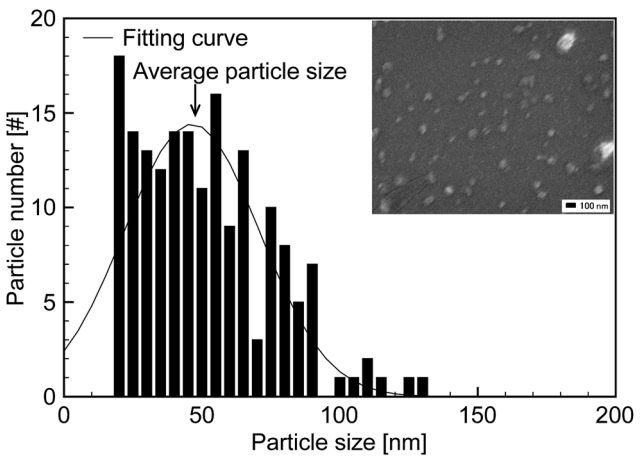

Fig. 2 Size distribution of particles deposited on a solid surface, and an electron micrograph of the particles (inset image).

and the number concentration of the particles of 11.6 #/μm^2 (Fig. 2).

Further, uniform deposition of Ag particles is necessary to measure a spatial distribution of target molecules, because the particle number in a laser spot can affect SERS.[17,18] Fig. 3 exhibits spacing between adjacent particles *versus* particle number being calculated by the image processing. This result shows an average spacing of around 100 nm, and a narrow distribution of the spacing, which ensures the uniformity. The present method can provide sub 100 nm resolution surface characterization. Enormous enhancement takes place from surface contact between adjacent particles at the distance of a single nanometer.[19] In our case, however, SERS arises from the particle/molecules/substrate interfaces.

Raman spectroscopic analysis

The coated surfaces in contact with Ag nanoparticles were characterized by Raman microscope (Nicolet Almega XR, Thermo Electron, Yokohama). An area of ~5 × 10^4 μm^2 was scanned with the step size of 20 μm. A laser of 532 nm with 10 mW was used as an excitation source. A laser spot diameter was 2 μm, meaning that around 36 Ag particles were simultaneously excited by a laser spot. Time and number of the exposures were set at 1 s and 10 times respectively. 250 spectra on average were approximately taken for each condition (*i.e.* substrate-lifting rate).

Deposited particles have a broad size distribution (Fig. 2), which might affect SERS signals derived from each particle. The size-dependent effect is not significant, because size of a laser spot diameter is much larger than that of particles. Furthermore, Ag particles tend to be easily oxidized in air and oxidation of Ag particles can affect SERS. A previous study reported that oxidation effect of Ag nanoparticles on SERS enhancement was moderate, when they were exposed to outdoor environment under sunlight for 4 hours.[20] In the present case, each experiment for substrate-lifting rate was conducted within 5 hours from deposition to SERS analysis. Furthermore, deposited particles were kept indoors so that the oxidation effect is negligible.

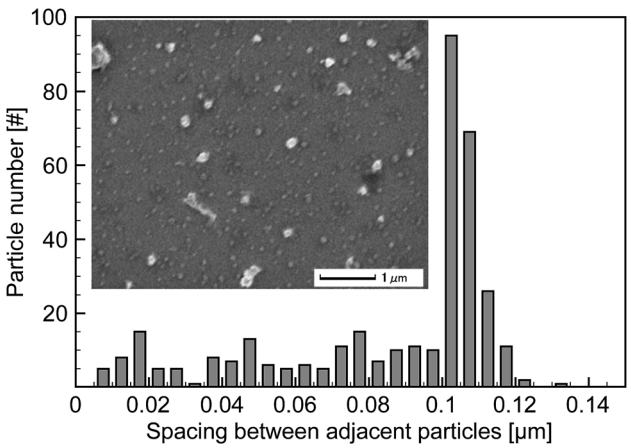

Fig. 3 Spacing between adjacent particles calculated from the images with deposited particles.

Results and discussion

Liquid and solid films

In a dip-coating method, evaporation rate of a contact line dominates size of the film and kinetics of the solidification on a substrate.[21,22] Evaporation is controllable by altering the substrate-lifting rate or a boiling point of solvent. Rapid evaporation, which is achievable with low boiling-point solvent, leads to solidification at a contact line between a solid substrate and liquid. This solidification rate is probably faster than the lifting rate so that the thickness of solid material can become thicker with decreasing in the rate.[23] In contrast, slow evaporation provides the opposite tendency,[24,25] because insufficient time for evaporation creates discontinuous islands of small drops.[22] In the present study, the latter case is applicable, because aqueous solution was used (Fig. 4). The size of liquid film then determines concentration of organic molecules that are left after solidification.

Thickness of liquid film, H is estimated to predict the molecular distribution on the substrate surface. The liquid film can be characterized with a substrate-lifting rate, U by the following equations[26]

$$H = 0.944 C_a^{\frac{1}{6}} (\eta U/\rho g)^{1/2} \quad (1)$$

$$C_a = \eta U/\sigma \quad (2)$$

where η, ρ and σ are the viscosity, the density and the surface tension of liquid, respectively, and g is the gravitational acceleration constant. eqn (1) is valid for C_a less than 10^{-3};[27] aqueous solution gives $C_a \ll 10^{-3}$ in the range of substrate-lifting rates (1 to 100 μm s^{-1}).

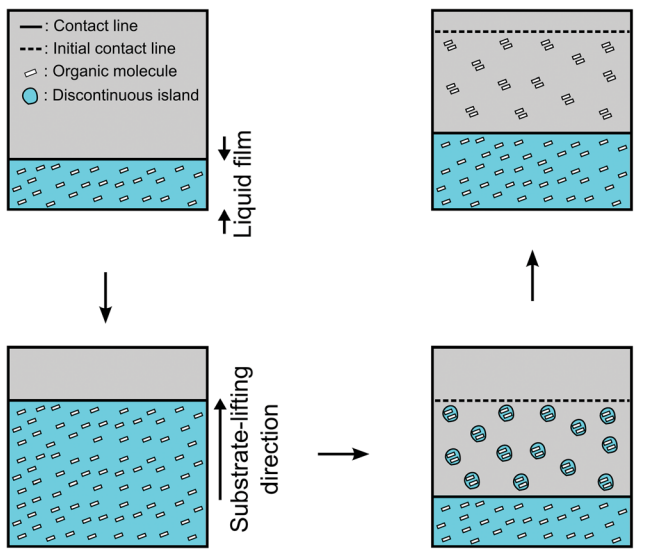

Fig. 4 A schematic illustration of development of discontinuous islands over a solid surface.

Thickness of solid film, h can be estimated on the basis of the mass balance between the solute concentration of the liquid film and the weight of the solid film.[28] When the width and length of liquid film are equal to those of solid film, the mass balance is described with the following equation,

$$h = (\rho_l/\rho_s) \times (w_l/100) \times H \quad (3)$$

where ρ_l and ρ_s are densities of bulk liquid (water) and solid (pesticide powder), and w_l is mass concentration in the liquid. Eqn (1) and (3) give the dependence of the substrate-lifting rate on the thickness of solid and liquid films (Fig. 5). The thickness of solid film is, however, physically impossible to be taken because the maximum value ($\sim$0.02 nm at $U = 100$ μm s^{-1}) is "smaller" than the minimum length of the N–H bond (*i.e.* $\sim$0.1 nm). The calculated results also support that the liquid film of target molecules cannot make dried layer(s) that covers the whole area of the substrate surface but discontinuous islands. Nonetheless the average mass concentration over unit area (g m^{-2}), C_m should increase with an increase in the substrate-lifting rate as described by the following form:

$$C_m = H \times w_l \times \rho_l \quad (4)$$

The thickness of liquid film is a function of the two-third power law of the substrate-lifting rate, $U^{2/3}$ according to eqn (1) and (2). Therefore, the concentration is directly proportional to the rate at a given concentration of solution: $C_m \sim U^{2/3}$.

Raman spectroscopy of coated surfaces after deposition of Ag nanoparticles

The target molecules on the surface were detected with the Raman microscope in the presence of Ag nanoparticles. Fig. 6 presents Raman mappings of the peak intensity at Raman band of 1558 cm^{-1} that can be attributed to the stretching vibration of the nitro group for $U = 1$ μm s^{-1} and $U = 100$ μm s^{-1} (a and b), representative spectra taken from the four measurement points (A to D) and illustrations of particle/substrate and particle/molecules/substrate interfaces on the points A and B. The color variation of each pixel of 20 × 20 μm^2 presents the extent of the intensity; as the color becomes darker, the intensity is higher. The number of the dark pixels becomes higher at $U = 100$ μm s^{-1} than at $U = 1$ μm s^{-1}. The spectral profile at 100 μm s^{-1} shows the specific peaks of 1558, 1976, 2119 and 2936 cm^{-1} as highlighted with dash lines, while the enhanced spectra (SERS spectra) at 1 μm s^{-1} is not frequently measurable. Since discontinuous layers of target molecules were formed and the particle number concentration was constant, the occurrence of SERS spectra depends on the existence of target molecules on the substrate in the measurement points (*i.e.* C_m, Fig. 6c).

With respect to the four peaks, we consider the average intensities, I and the occurrence frequency of SERS which is defined as the ratio of the number of SERS spectra to that of total spectra, R. Fig. 7 shows plots of the intensities and the ratios *versus* C_m. The average intensity was found to be independent of C_m (Fig. 7a) because of the two reasons: (i) the particle number concentrations (spraying times) are constant for each substrate-lifting rate, and (ii) enhanced Raman intensity depends on the number of individual particles under a laser spot.[17,18] Although the neighboring distance between particles at a single nanometer, or hot spots is also related to the enhancement,[19] the effect is negligible in the present study because the distance is around 100 nm (Fig. 3) and further, target molecules do not exist between adjacent particles (Fig. 6c). In contrast, the values of R are positively correlated to C_m at the feature peaks. Plots of R *versus* C_m (Fig. 7b) give regression lines, providing high correlations; the coefficients of

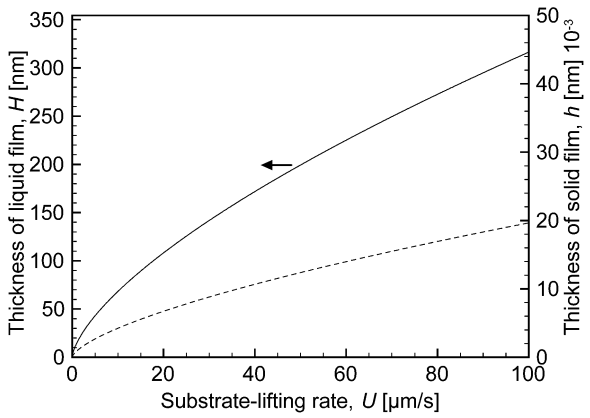

Fig. 5 Calculated thickness of liquid and solid films, H and h *versus* substrate-lifting rates.

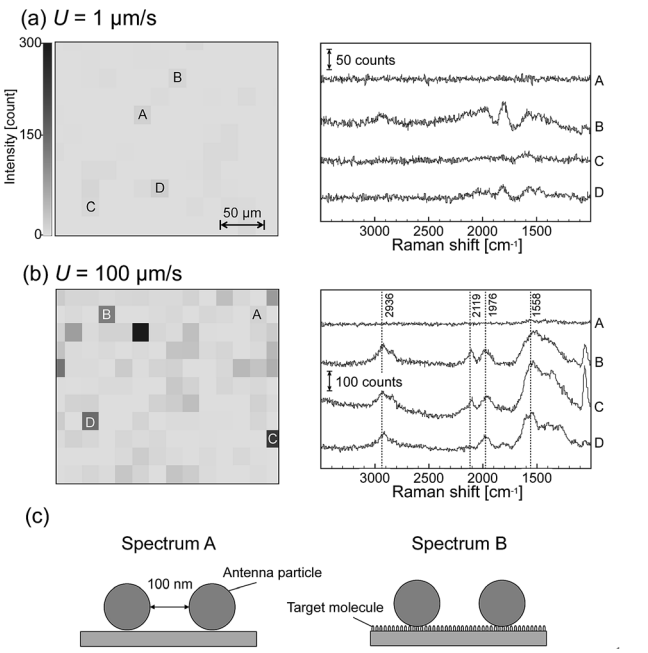

Fig. 6 Raman mappings (left) of peak intensities at 1558 cm^{-1} for the substrate-lifting rate (U) of 1 (a) and 100 (b) μm s^{-1} and Raman spectra obtained from each measurement point (A to D, right). Formation of particle/substrate (spectrum A) and particle/molecules/substrate interfaces (c).

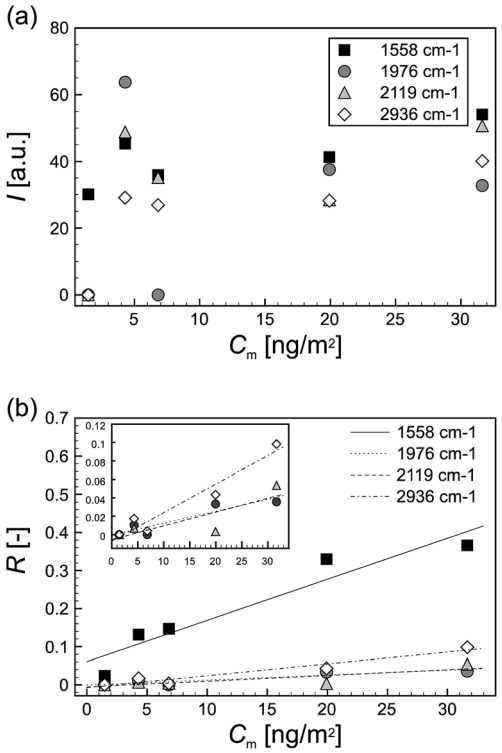

Fig. 7 Average Raman intensity, I (a) and occurrence frequency, R (b) with respect to peaks of 1558, 1976, 2119 and 2936 cm^{-1} *versus* mass concentration per unit area, C_m (*i.e.* $\sim U^{2/3}$); the regression lines are described for each peak.

determine are calculated to be 0.91, 0.85, 0.69 and 0.94 for the specific peaks of 1558, 1976, 2119 and 2936 cm^{-1} respectively. The results imply that the occurrence frequency (R) becomes an index to measure the mass concentration of the target molecules on a solid surface in the presence of enhancer nanoparticles. Further, I and R reach zero values on $U = 1$ μm s^{-1} (*i.e.* $C_m = 1.47$ ng m^{-2}) except the peak of 1558 cm^{-1}. The proposed method, therefore, provides the applicability of gas-phase nanoparticles to SERS technique with the detection limit above ~1.47 ng m^{-2} (*i.e.* 3.54 molecule per μm^2) and this limit can be tuned by controlling the particle number concentration.

Applicability of particle deposition to any surface

The electrostatic spray enables stable deposition of particles under given electric fields. For instance, charged particles less than 1 μm are predominantly influenced by electrostatic deposition.[29] Charged Ag nanoparticles can be deposited on a silicon substrate as well as non-conductive substrates. To prove the applicability of electrostatic deposition to non-conductive substrates, we conducted an electrodynamic numerical simulation (using a commercial FEM-based software, COMSOL Multiphysics 4.3, Stockholm) with either silicon or non-conductive glass substrates (see the ESI†). The calculations revealed that the surface electric fields of the substrates are comparable. This suggested that the deposition of particles is independent of the substrates electrical properties because electrostatic deposition is determined by electric fields. Therefore, the proposed method could be practical for any surface. The further applications of the proposed method in analysing the different morphologies of surfaces (*e.g.* pesticide residues on vegetation, bees or soils) will be presented in future studies.

Conclusions

A spatial distribution of organic molecules on a solid surface was directly measured using a gas-phase nanoparticle route assisted SERS method with the detection limit above ~3.54 molecule per μm^2. SERS spectra yielded the following results: the average peak intensity of SERS spectra and the occurrence frequency of SERS for the feature peaks *versus* the mass concentration of target molecules. The occurrence frequency was positively correlated to the two-third power law of the lifting rates in relation to the mass concentrations of the target molecules altered by a dip-coating method. The intensities were found to be independent of the mass concentration. The regression lines between the occurrence frequency and the rates give high correlations, suggesting that the values of the ratio can be used to measure the mass concentration of organic molecules existed on a solid surface.

Acknowledgements

The authors gratefully thank M. Iijima, M. Tsukada, H. Kamiya, and H. Kakuta for the valuable comments, M. Horio for the instrument of Raman spectroscopy and C. Hayashi (passed away in 2010) for guiding us to this research field. This work was supported by Ministry of Education, Culture, Sports, Science and Technology MEXT Kakenhi Grant (no. 20120010), and JSPS Kakenhi Grant (no. 23560904, 26420761, 23246132).

Notes and references

1 C. Vericat, M. E. Vela and R. C. Salvarezza, *Phys. Chem. Chem. Phys.*, 2005, **7**, 3258–3268.
2 P. K. Chu and L. Li, *Mater. Chem. Phys.*, 2006, **96**, 253–277.
3 B. L. Frey and R. M. Corn, *Anal. Chem.*, 1996, **68**, 3187–3193.
4 M. Futamata, Y. Maruyama and M. Ishikawa, *J. Mol. Struct.*, 2005, **735–736**, 75–84.
5 J. F. Li, Y. F. Huang, Y. Ding, Z. L. Yang, S. B. Li, X. S. Zhou, F. R. Fan, W. Zhang, Z. Y. Zhou, D. Y. Wu, B. Ren, Z. L. Wang and Z. Q. Tian, *Nature*, 2010, **464**, 392–395.
6 J. Vongsvivut, E. G. Robertson and D. McNaughton, *J. Raman Spectrosc.*, 2010, **41**, 1137–1148.
7 D. L. Jeanmaire and R. P. Van Duyne, *J. Electroanal. Chem. Interfacial Electrochem.*, 1977, **84**, 1–20.
8 M. G. Albrecht and J. A. Creighton, *J. Am. Chem. Soc.*, 1977, **99**, 5215–5217.
9 K. Kneipp, Y. Wang, H. Kneipp, L. T. Perelman, I. Itzkan, R. R. Dasari and M. S. Feld, *Phys. Rev. Lett.*, 1997, **78**, 1667–1670.
10 J. Jiang, K. Bosnick, M. Maillard and L. Brus, *J. Phys. Chem. B*, 2003, **107**, 9964–9972.

11 V. K. Jha and D. S. Wydoski, *U.S. Geological Survey*, Colorado, 2003.
12 M. Gen, H. Kakuta, Y. Kamimoto and I. W. Lenggoro, *Jpn. J. Appl. Phys.*, 2011, **50**, 06GG10.
13 Y. Xie, G. Mukamurezi, Y. Sun, H. Wang, H. Qian and W. Yao, *Eur. Food Res. Technol.*, 2012, **234**, 1091–1098.
14 B. Liu, P. Zhou, X. Liu, X. Sun, H. Li and M. Lin, *Food Bioprocess Technol.*, 2013, **6**, 710–718.
15 B. Liu, G. Han, Z. Zhang, R. Liu, C. Jiang, S. Wang and M.-Y. Han, *Anal. Chem.*, 2012, **84**, 255–261.
16 P. C. Lee and D. Meisel, *J. Phys. Chem.*, 1982, **86**, 3391–3395.
17 C. J. L. Constantino, T. Lemma, P. A. Antunes and R. Aroca, *Anal. Chem.*, 2001, **73**, 3674–3678.
18 R. P. Paradkar and R. R. Williams, *Anal. Chem.*, 1994, **66**, 2752–2756.
19 K. L. Wustholz, A.-I. Henry, J. M. McMahon, R. G. Freeman, N. Valley, M. E. Piotti, M. J. Natan, G. C. Schatz and R. P. Van Duyne, *J. Am. Chem. Soc.*, 2010, **132**, 10903–10910.
20 Y. Han, R. Lupitskyy, T.-M. Chou, C. M. Stafford, H. Du and S. Sukhishvili, *Anal. Chem.*, 2011, **83**, 5873–5880.
21 D. Qu, E. Ramé and S. Garoff, *Phys. Fluids*, 2002, **14**, 1154–1165.
22 L. Li, P. Gao, K. C. Schuermann, S. Ostendorp, W. Wang, C. Du, Y. Lei, H. Fuchs, L. D. Cola, K. Müllen and L. Chi, *J. Am. Chem. Soc.*, 2010, **132**, 8807–8809.
23 J. Jang, S. Nam, K. Im, J. Hur, S. N. Cha, J. Kim, H. B. Son, H. Suh, M. A. Loth, J. E. Anthony, J.-J. Park, C. E. Park, J. M. Kim and K. Kim, *Adv. Funct. Mater.*, 2012, **22**, 1005–1014.
24 M. Guglielmi, P. Colombo, F. Peron and L. Mancinelli Degli Esposti, *J. Mater. Sci.*, 1992, **27**, 5052–5056.
25 P. Yimsiri and M. R. Mackley, *Chem. Eng. Sci.*, 2006, **61**, 3496–3505.
26 L. Landau and B. Levich, *Acta Physicochim. URSS*, 1942, **17**, 42–54.
27 P. Groenveld, *Chem. Eng. Sci.*, 1970, **25**, 33–40.
28 C. Jing, X. Zhao and H. Tao, *Surf. Coat. Technol.*, 2006, **201**, 2655–2661.
29 M. Gen, S. Ikawa, S. Sagawa and I. W. Lenggoro, *e-J. Surf. Sci. Nanotechnol.*, 2014, **12**, 238–241.